Supplementary Material (ESI) for Dalton Transactions

Supporting Information

A new polyoxometalate-based 3d-4f heterometallic aggregate: a model for the design and synthesis of new heterometallic clusters

Weilin Chen, Yangguang Li,* Yonghui Wang, Enbo Wang* and Zhiming Zhang

Synthetic discussion:

So far, most huge POM-based clusters were prepared by virtue of a straightforward "one-pot" synthesis process or a "step-by-step" building-block approach.[1-3] Compound **1** was prepared with the "one-pot" synthesis route, however, this synthetic process also involves in the formation of lacunary polyoxoanion building blocks. In the first step, the mixture of $Na_2WO_4{\cdot}2H_2O$, $Na_2HAsO_4{\cdot}7H_2O$ and 6M HCl in aqueous solution with very low pH value (less than 1.0) is inclined to form the $[\alpha\text{-}AsW_{12}O_{40}]^{3-}$ Keggin-type precursor. In the following step, the adjustment of the pH value of the reaction system with KOH may lead to the partial decomposition of the $[\alpha\text{-}AsW_{12}O_{40}]^{3-}$ to the $\{\alpha\text{-}AsW_{10}\}$ units. During the preparation of **1**, three factors should be emphasized. Firstly, the final pH value of the reaction system should be kept in the pH range of 4.0 ~ 5.0. It is presumed that the divacant Keggin-type species $[\alpha\text{-}AsW_{10}O_{38}]^{11-}$ might be stable in this pH range, since no crystalline phase was obtained out of this pH range. Secondly, the introduction of hexamethylenetetramine (HMTA) plays an important role for the isolation of **1**. Attempts to use other organic amines such as piperazine and triethylamine as substitutes for HMTA cannot obtain the polyoxoanion of **1**. Interestingly, the HTMA changes into $[HMTA\text{-}CH_3]^+$ cation during the reaction, which may results from the acid-catalytic decomposition of some HMTA molecules and lead to a succedent alkylation of HMTA in solution.[4] Thirdly, the use of KOH seems to not only play a role in adjusting the pH value of the whole reaction system, but also introducing a suitable cationic template for the assembly of the polyoxoanion of **1**. During the synthesis, if KOH was substituted to NaOH, no crystals were isolated. Thus, the cationic template seems to be necessary for the synthesis of POM-based

high-nuclear clusters.[5]

Furthermore, considering that the initial materials of $Na_2HAsO_4 \cdot 7H_2O$ is virulent and hard to obtain, we improve the synthesis with an exchengeable method as follows: a solution of $Na_2WO_4 \cdot 2H_2O$ (3.30g, 10mmol) and $NaAsO_2$ (0.13g, 1mmol) in water (30 mL) was acidified with 6M HCl (3 mL, 18 mmol). Then, $(NH_4)_2Ce(NO_3)_6$ (1.096 g, 2mmol) and HMTA (0.14g, 1 mmol) in water (15 mL), and the solid of $FeCl_3 \cdot 6H_2O$ (0.54 g, 2mmol) was added to above solution successively. The pH of the resulting cloudy solution was adjusted to 4~5 by the addition of 1M KOH and heated to 85~95°C for 4 h. After being cooled to room temperature, the brown suspension was filtered. The filtrate was kept at room temperature. The brown crystalline products were isolated after one month (Yield: 60 % based on W). The IR spectrum and the single-crystal X-ray diffraction confirm that the brown compound is **1**. It is noteworthy that the redox reaction between $As^{III}O_2^-$ and Ce^{IV} ions occurs, leading to the final As^V and Ce^{III} oxidation states in the final crystal structure.

References

1 A. Müller, B.Botar, S. K.Das, H. Bögge, M. Schmidtmann and A. Merca, *Polyhedron*, 2004, **23**, 2381; K. Wassermann, M. H. Dickman and M. T. Pope, *Angew. Chem. Int. Ed. Engl.*, 1997, **36**, 1445.

2 N. L. Laronze, M.Haouas, J.Marrot, F. Taulelle and G.Hervé, *Angew. Chem. Int. Ed.*, 2006, **45**, 139; U. Kortz, M. G. Savelieff, B. S. Bassil and M. H. Dickman, *Angew. Chem. Int. Ed.*, 2001, **40**, 3384.

3 W. L. Chen, Y. G. Li, Y. H. Wang, E. B. Wang and Z. M. Su, *Dalton Trans.*, 2007, 4293.

4 D. L. Long, Paul Kögerler, L. J. Farrugia and L. Cronin, *Angew. Chem. Int. Ed.*, 2003, **42**, 4180; D. L. Long, O. Brücher, C. Streb and L. Cronin, *Dalton Trans.*, 2006, 2852; D. L. Long, P. Kögerler, L. J. Farrugiaa and L. Cronin, *Dalton Trans.*, 2005, 1372; T. Duraisamy, Nishma Ojha, A. Ramanan and J. J. Vittal, *Chem. Mater.*, 1999, **11**, 2339.

5 D. L. Long, H. Abbas, P. Kogerler and L. Cronin, *J. Am. Chem. Soc.*, 2004, **126**, 13880; K. Fukaya and T. Yamase, *Angew. Chem. Int. Ed.*, 2003, **42**, 654; H. G. Anga, W. Fraenkb, K. Karaghiosoffb, T. M. Klapötkeb, H. Nöthb, J. Sprottb, M. Suterb, M. Vogtb and M. Warchholdb, *Z. Anorg. Allg. Chem.*, 2002, **628**, 2901; H. Xue, H. X. Gao, B. Twamley and J. M. Shreeve, *Eur. J. Inorg. Chem.*, 2006, 2959.

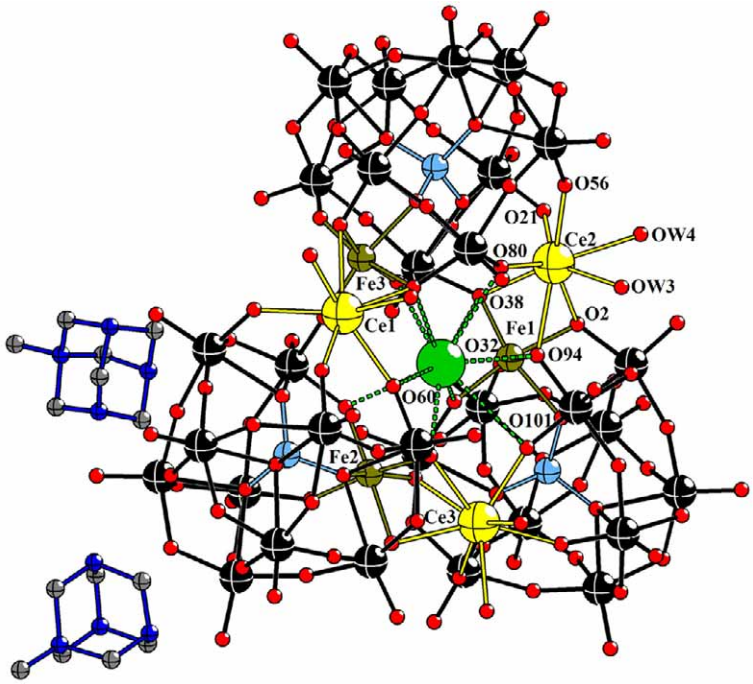

Fig. S1. Ball-and-stick representation of **1**, Color codes: W (black), Ce (yellow), As (light blue), Fe (brown), K (green), O (red), C (grey), N (blue). Counter-cations K^+ and Na^+ and solvent water molecules are omitted. H atoms on C atoms are also omitted for clarity.

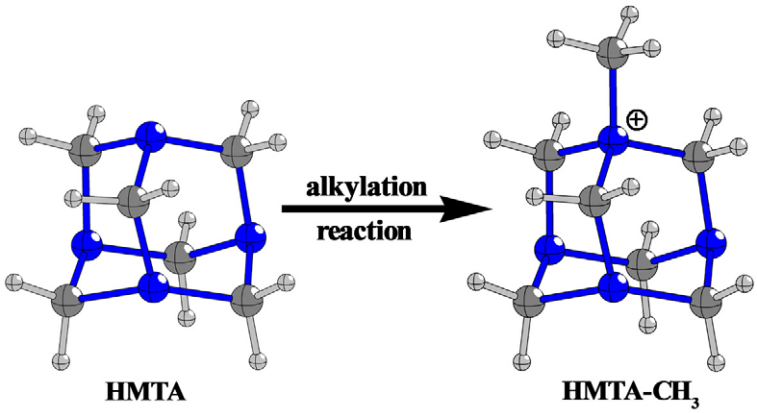

Scheme S1. Schematic view of the structural transformation from HMTA to HMTA-CH_3 *via* the alkylation reaction.

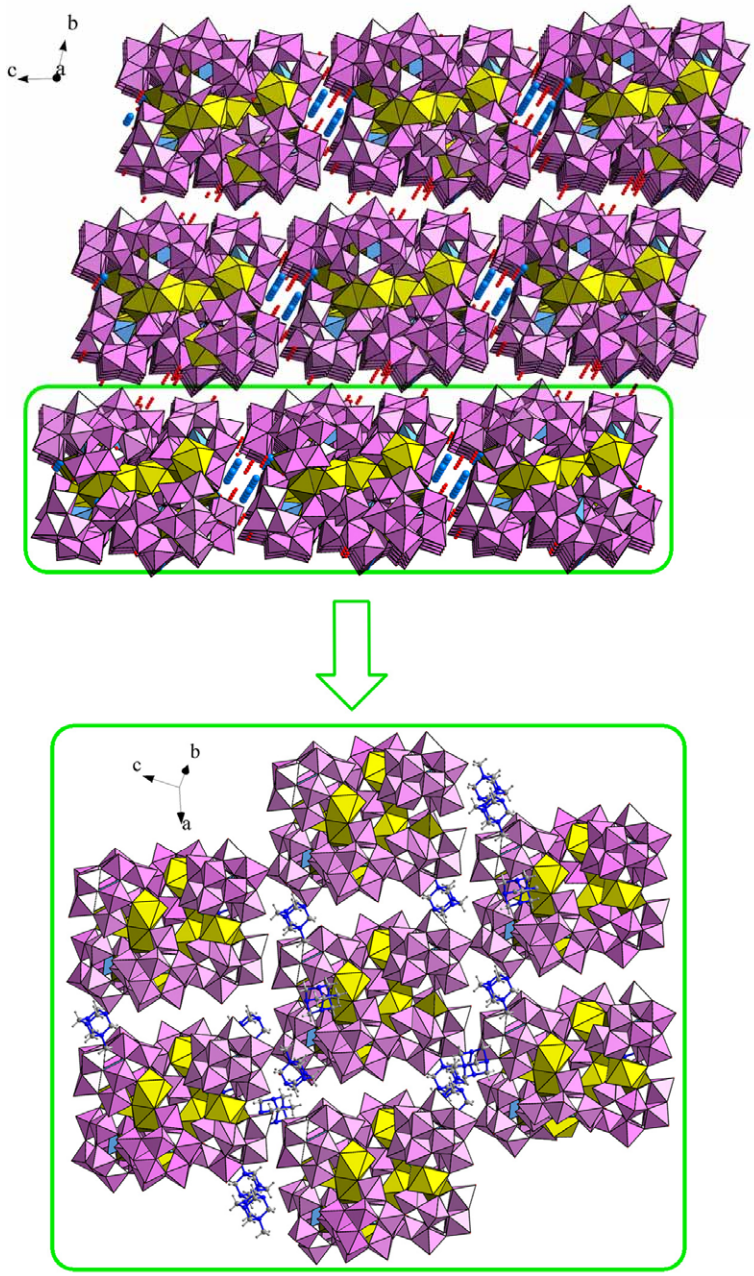

Fig. S2. (top) The packing arrangement of **1** viewed along *a* axis (the HMTA-CH_3 cations, solvent water molecules and the bonds of K-O, Na-O are omitted for clarity); **(below)** the packing view of one layer on the [010] plane (the solvent water molecules and K^+, Na^+ cations are omitted for clarity). The polyanions are represented with polyhedra; K and Na ions are shown with balls. K (blue), Na (green).

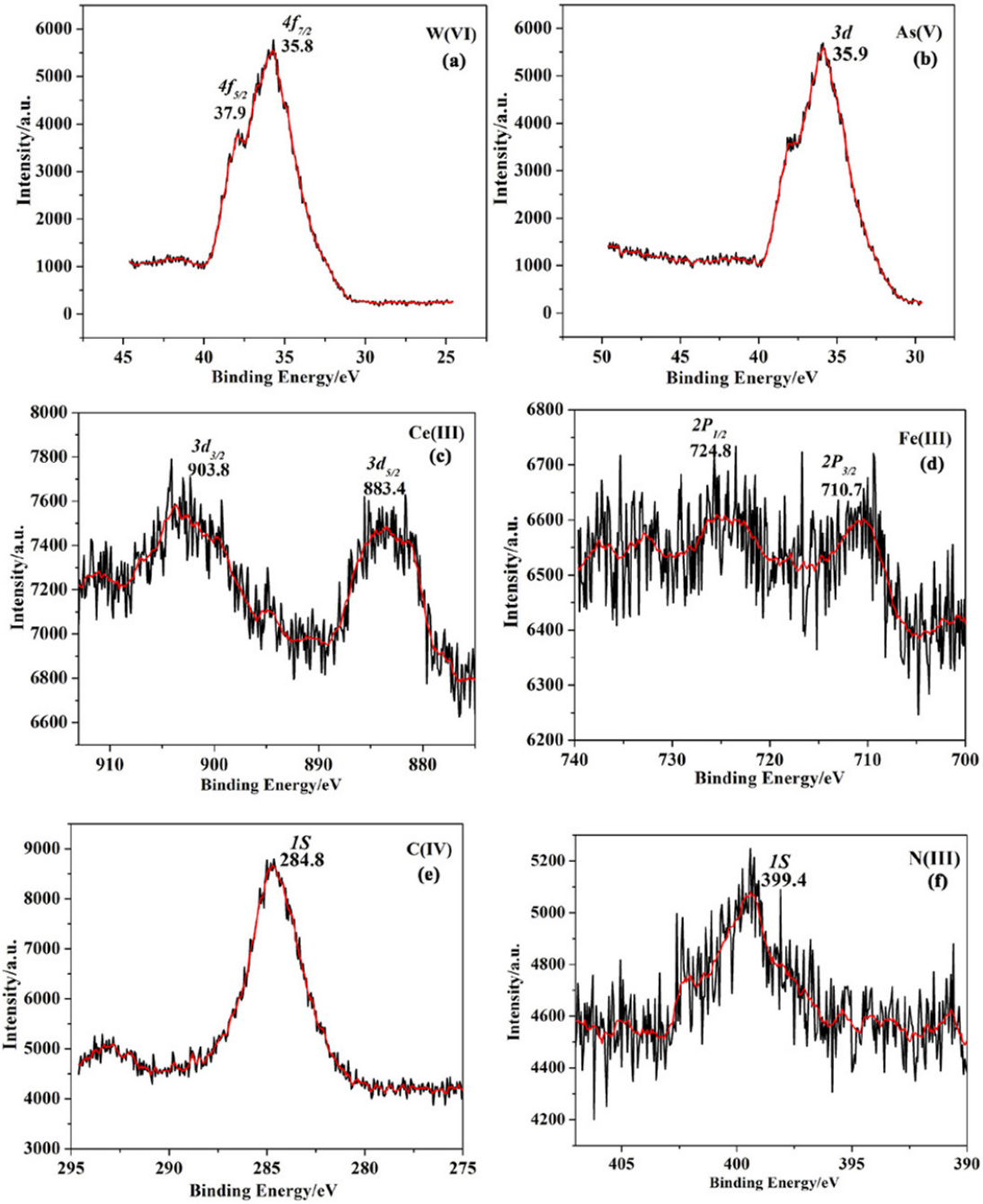

Fig. S3. The XPS spectra of W4f, As3d, Ce3d, Fe2p, C1s and N1s for **1.**

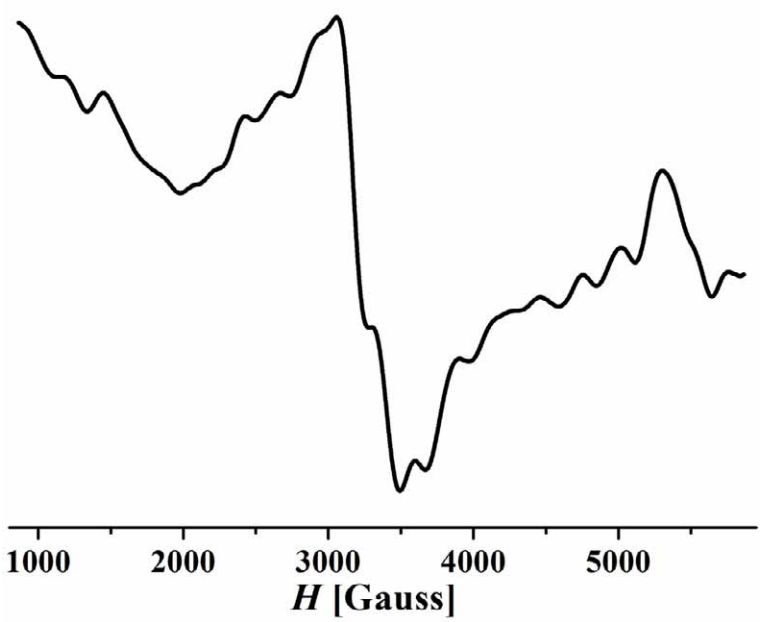

Fig. S4. The EPR spectrum of **1**. The EPR spectrum of **1** at room temperature shows a wide Fe^{3+} signal with $g_{\parallel} = 2.1756$ and $g_{\perp} = 2.0283$, which is a little lower than the g value of a high spin ferric (Fe^{3+}; S=5/2) center. It is possible that the g value of a high spin Fe^{3+} is reduced by the antiferromagnetic coupling between Fe^{3+} (S=5/2) and Ce^{3+} (S=1/2) center.

Fig. S5. Photograph of the Sephadex G-50 column. Two distinct colored bands corresponding to $[P_2W_{15}Mo_2VO_{62}]^{8-}$ (dark blue) and **1** (yellow) have already separated.

Gel filtration chromatography is a reliable technique to estimate the molecular mass.[1] So it was used to check whether **1** exists as a trimer, a dimer or perhaps as a monomer in solution in this investigation in order to establish if **1** is stable in the solution. A gel filtration chromatography analysis was carried out with a 1 mL mixture of 1 mM each of $[P_2W_{15}Mo_2VO_{62}]^{8-}$($Mo_2VP_2W_{15}$) and $[HMTA\text{-}CH_3]_2K_{3.5}Na_{8.5}[K\subset\{FeCe(AsW_{10}O_{38})(H_2O)_2\}_3]\bullet\sim 36H_2O$ (**1**) in a 0.5 M $H_2SO_4/NaSO_4$ (pH=4.33) solution (being the buffers used in the electrochemical experiments and UV-vis spectrum) passing

through a 40 cm×1 cm^2 Sephadex G-50 fine column previously equilibrated in the same solution. Sephadex G-50 separates molecules ranging in molecular mass from 500 to 10000, the largest being eluted first. The migration and concomitant separation of the colored products (**1**, yellow and $Mo_2VP_2W_{15}$, blue) down the column was easily followed by visual inspection. Approximately 2 mL solution were collected and analyzed by UV-Vis spectrophotometry, which shows that the two products each have its characteristic spectrum with strong absorption bands in the UV region in the mixture. The same procedure was repeated in pure water with a 1 mL mixture of 1 mM each of **1** and $Mo_2VP_2W_{15}$, the result being the same as for the experiment in 0.5 M $H_2SO_4/NaSO_4$ (pH=4.33) solution. [2-4]

The gel filtration chromatography analysis reveals that **1** eluted faster than $[P_2W_{15}Mo_2VO_{62}]^{8-}$ (ionic mass = 4055). This indicates that the molecular masses of $[\{FeCe(AsW_{10}O_{38})(H_2O)_2\}_3]^{15-}$ (**1**) (ionic masses= 8260) are quite different from that of $[P_2W_{15}Mo_2VO_{62}]^{8-}$ and rules out the possibility of **1** breaking down into one dimers, one monomers and mixtures of the two. If **1** were indeed the dimers in the solution, they have ionic masses of 4130 g/mol, close to that of $[P_2W_{15}Mo_2VO_{62}]^{8-}$, which would elute closer together. If polyoxoanions **1** fall apart, resulting in monomers, they have the ionic masses of 2753, and therefore would elute later.

References:

(1) Nelson, D. L.; Cox, M. M.; Lehninger, A. L. Principles of Biochemistry, 3rd ed.; Worth Publishers: New York, 2000.
(2) B. S. Bassil, U. Kortz, A. S. Tigan, J. M. Clemente-Juan, B. Keita; P. Oliveira, L. Nadjo, *Inorg. Chem.*, 2005, **44**, 9360.
(3) B. Keita,P. de Oliveira, L. Nadjo and U. Kortz, *Chem. Eur. J.*, 2007, **13**, 5480.
(4) Z. M. Zhang, Y. F. Qi, C. Qin, Y. G. Li, E. B. Wang, X. L. Wang, Z. M. Su and L. Xu, *Inorg. Chem.*, 2007, **46**, 8162.

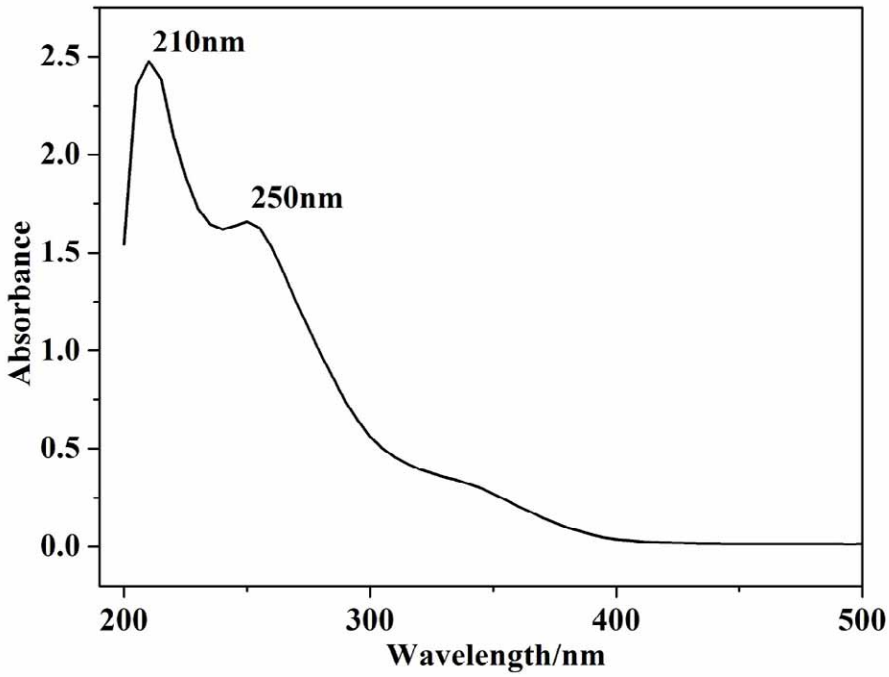

Fig. S6. The UV-vis spectrum of the sample in the H_2SO_4/Na_2SO_4 solution for **1** at pH = 4.33.

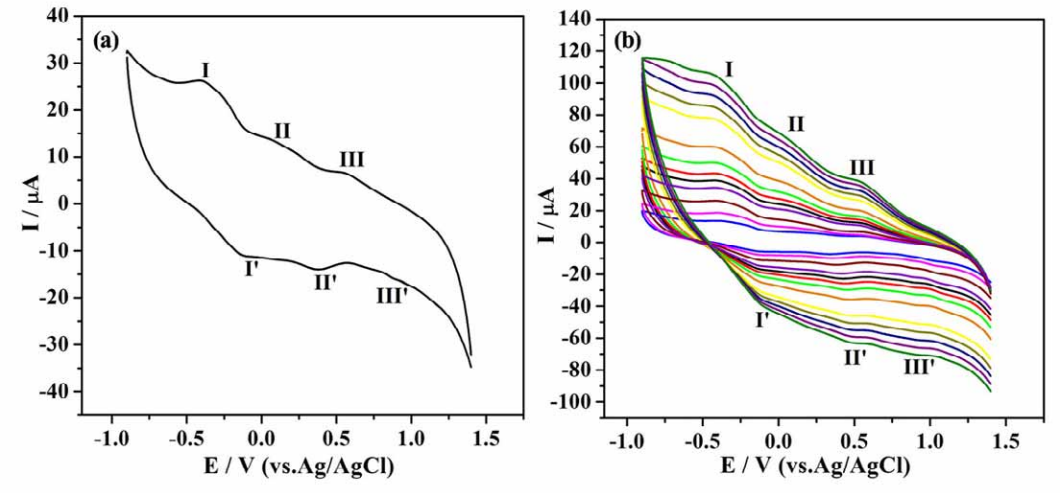

Fig. S7. (a) Cyclic voltammograms (CV) for 1 mM sample of **1** in 0.5 M H_2SO_4/Na_2SO_4 at pH = 4.33. Working electrode: glassy carbon; Reference electrode: Ag/AgCl; Scan rate: 50 mVs^{-1}. **(b)** CV of **1** in the 0.5 M H_2SO_4/Na_2SO_4 at pH = 4.33 at different scan rates (from inner to outer: 20, 30, 50, 80, 100, 120, 150, 200, 250, 300, 350, 400, 450, 500 mVs^{-1}).

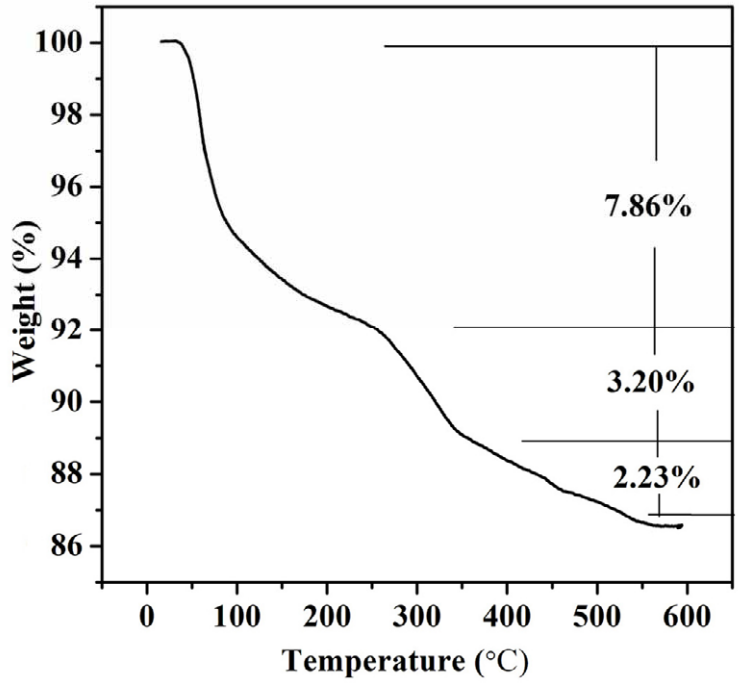

Fig. S8. TG curve of **1.** The TG curve shows three continual weight losses. The first weight loss is in the temperature range of 50 ~ 250 °C, corresponding to the loss of all lattice and coordinated water molecules in **1**. The value of ca. 7.86 % is in accordance with the calculated value of 7.89 % (~42H_2O). The second weight loss in the temperature range of 250 ~ 360 °C is attributed to the loss of all {HMTA-CH_3} organic cations. The value of 3.20 % is close to the calculated value of 3.24 %. The third weight loss step of ca. 2.23 % in the range of 360~ 550 °C might be the decomposition of partial arsenic oxide from the residue.

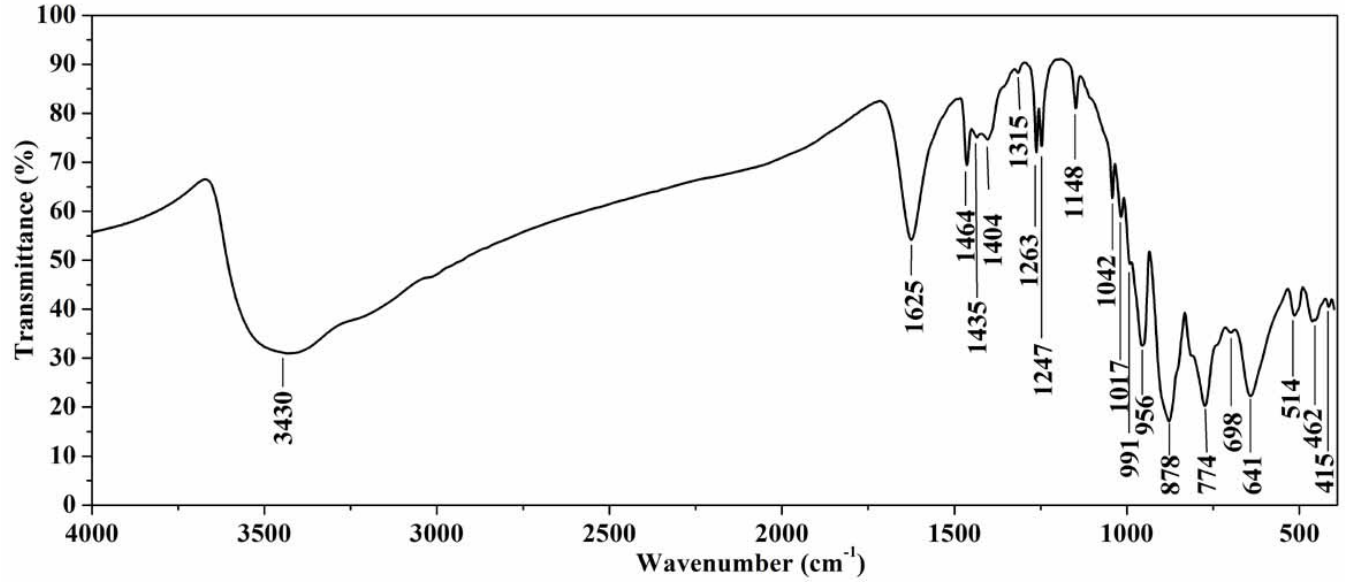

Fig. S9. IR spectrum of **1** The characteristic peaks at 956, 878, 774 and 641 cm^{-1} are ascribed to vibrations of ν(As–O), ν(W=Od), ν(W–Ob) and ν(W–Oc), respectively. The broad peak at 3430 cm^{-1} and the strong peak at 1625 cm^{-1} are attributed to the lattice water molecules and aqua ligands. The strong bands at 1464, 1263, 1247 and 1148 cm^{-1} are assigned to {HMTA-CH_3} organic molecules.

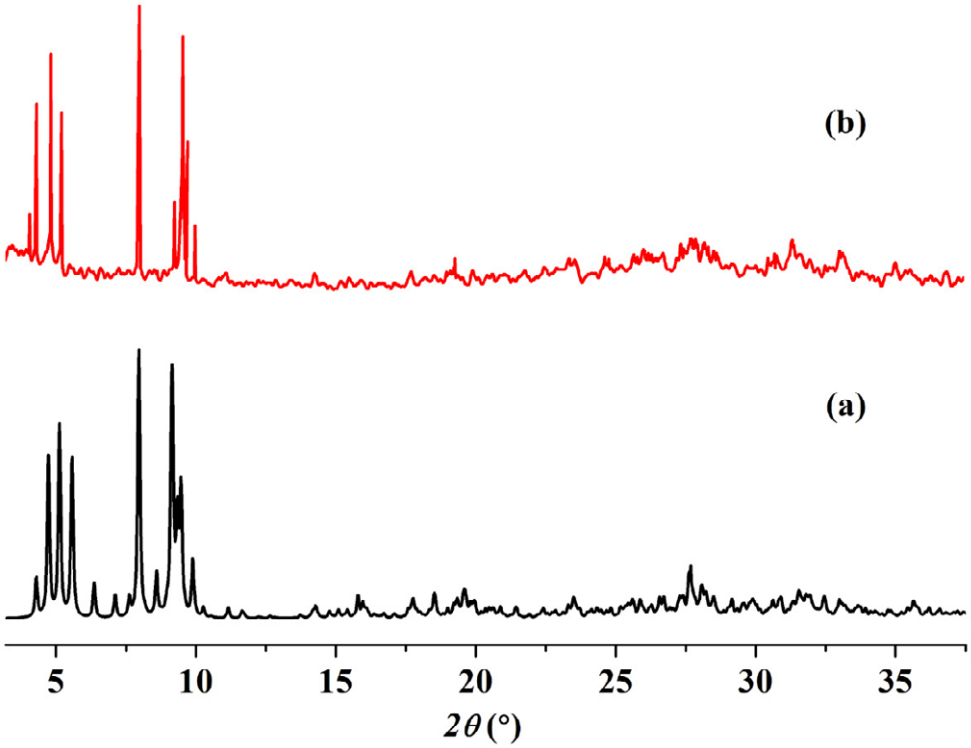

Fig. S10. Simulated and experimental XRPD patterns of **1**. (a) simulated XRPD; (b) XRPD at room temperature (r. t.). The peak positions of simulated and experimental XRPD pattern at r. t. are in agreement with each other, indicating the good phase purity of the compound. The differences in intensity may be due to the preferred orientation of the crystalline powder samples.

Table S1 Crystal Data and Structure Refinement for **1**

	1
Empirical formula	$C_{14}H_{114}N_8O_{156}As_3Ce_3Fe_3K_{4.5}Na_{8.5}W_{30}$
M	9590.67
λ/Å	0.71073Å
T/K	293(2)
Crystal dimensions/mm	0.28 × 0.26 × 0.22
Crystal system	Triclinic
Space group	$P\bar{1}$
a/Å	19.9015(15)
b/Å	20.1830(15)
c/Å	22.7851(17)
α/°	95.7770(10)
β/°	111.6020(10)
γ/°	107.6850(10)
V/Å^3	7870.5(10)
Z	2
D_c/Mg m^{-3}	4.047
μ/mm^{-1}	23.826
F(000)	8504
θ Range/°	1.64–25.00
Measured reflections	39904
Independent reflections	27359
Data/restraints/parameters	27359/132/1190
R_{int}	0.0591
$R_1(I > 2\sigma(I))$ [a]	0.0617
wR_2 (all data) [a]	0.1743
Goodness-of-fit on F^2	1.007
$\Delta\rho_{max, min}$/ e Å^{-3}	3.709, -4.507

[a] $R1 = \sum||F_0|-|F_C||/\sum|F_0|$; $wR_2 = \sum[w(F_0^2-F_C^2)^2]/\sum[w(F_0^2)^2]^{1/2}$

Table S2. Selected bond lengths (Å) and bond angles(º) of **1**

W(1)-O(11)	1.69(2)	W(2)-O(93)	1.705(16)	W(3)-O(9)	1.713(19)
W(1)-O(5)	1.852(16)	W(2)-O(46)	1.845(17)	W(3)-O(53)	1.833(17)
W(1)-O(18)	1.854(17)	W(2)-O(27)	1.861(16)	W(3)-O(24)	1.918(16)
W(1)-O(71)	1.929(17)	W(2)-O(31)	1.994(15)	W(3)-O(104)	1.939(16)
W(1)-O(41)	1.959(17)	W(2)-O(26)	2.003(17)	W(3)-O(76)	1.964(19)
W(1)-O(42)	2.482(18)	W(2)-O(45)	2.384(16)	W(3)-O(43)	2.360(17)
W(4)-O(15)	1.733(18)	W(5)-O(17)	1.71(2)	W(6)-O(95)	1.742(18)
W(4)-O(50)	1.734(17)	W(5)-O(63)	1.757(17)	W(6)-O(32)	1.802(15)
W(4)-O(47)	1.884(15)	W(5)-O(16)	1.902(17)	W(6)-O(57)	1.877(17)
W(4)-O(39)	1.976(16)	W(5)-O(20)	1.968(18)	W(6)-O(28)	1.926(17)
W(4)-O(18)	2.065(17)	W(5)-O(112)	2.053(15)	W(6)-O(64)	2.010(16)
W(4)-O(42)	2.378(17)	W(5)-O(114)	2.375(18)	W(6)-O(51)	2.377(17)
W(7)-O(23)	1.727(18)	W(8)-O(65)	1.716(15)	W(9)-O(107)	1.696(17)
W(7)-O(80)	1.766(16)	W(8)-O(37)	1.868(17)	W(9)-O(30)	1.812(16)
W(7)-O(62)	1.900(17)	W(8)-O(86)	1.868(19)	W(9)-O(38)	1.883(17)
W(7)-O(81)	2.002(18)	W(8)-O(3)	1.973(18)	W(9)-O(106)	1.931(17)
W(7)-O(37)	2.055(16)	W(8)-O(36)	1.993(18)	W(9)-O(97)	1.989(17)
W(7)-O(25)	2.397(17)	W(8)-O(25)	2.438(16)	W(9)-O(59)	2.391(15)
W(10)-O(89)	1.728(17)	W(11)-O(8)	1.687(18)	W(12)-O(84)	1.706(18)
W(10)-O(110)	1.752(18)	W(11)-O(60)	1.796(17)	W(12)-O(56)	1.754(16)
W(10)-O(94)	1.844(17)	W(11)-O(73)	1.866(16)	W(12)-O(81)	1.863(18)
W(10)-O(34)	1.990(15)	W(11)-O(57)	1.961(16)	W(12)-O(113)	2.006(18)
W(10)-O(55)	2.067(16)	W(11)-O(16)	1.964(17)	W(12)-O(77)	2.045(17)
W(10)-O(101)	2.410(15)	W(11)-O(114)	2.382(18)	W(12)-O(35)	2.375(16)
W(13)-O(85)	1.757(19)	W(14)-O(7)	1.700(18)	W(15)-O(69)	1.730(18)
W(13)-O(21)	1.772(18)	W(14)-O(2)	1.827(17)	W(15)-O(87)	1.874(17)
W(13)-O(97)	1.899(17)	W(14)-O(55)	1.837(15)	W(15)-O(20)	1.880(18)
W(13)-O(54)	1.995(18)	W(14)-O(29)	1.955(16)	W(15)-O(102)	1.926(19)
W(13)-O(105)	2.016(17)	W(14)-O(111)	1.983(19)	W(15)-O(19)	1.941(16)
W(13)-O(59)	2.316(15)	W(14)-O(101)	2.451(16)	W(15)-O(22)	2.335(16)
W(16)-O(74)	1.706(17)	W(17)-O(91)	1.748(18)	W(18)-O(52)	1.727(19)
W(16)-O(88)	1.800(18)	W(17)-O(1)	1.820(16)	W(18)-O(49)	1.816(16)
W(16)-O(39)	1.900(16)	W(17)-O(26)	1.848(17)	W(18)-O(108)	1.904(18)
W(16)-O(33)	1.996(16)	W(17)-O(24)	1.954(17)	W(18)-O(106)	1.922(17)
W(16)-O(82)	2.088(17)	W(17)-O(68)	1.983(19)	W(18)-O(100)	1.992(19)
W(16)-O(61)	2.378(16)	W(17)-O(43)	2.381(16)	W(18)-O(4)	2.410(15)
W(19)-O(90)	1.719(19)	W(20)-O(10)	1.71(2)	W(21)-O(72)	1.709(18)
W(19)-O(104)	1.889(16)	W(20)-O(98)	1.878(19)	W(21)-O(75)	1.772(17)
W(19)-O(44)	1.902(18)	W(20)-O(29)	1.906(16)	W(21)-O(34)	1.878(15)
W(19)-O(83)	1.916(19)	W(20)-O(28)	1.918(17)	W(21)-O(67)	2.024(16)
W(19)-O(33)	1.920(15)	W(20)-O(13)	1.938(19)	W(21)-O(87)	2.043(17)
W(19)-O(61)	2.332(16)	W(20)-O(51)	2.415(17)	W(21)-O(22)	2.373(16)
W(22)-O(12)	1.736(19)	W(23)-O(14)	1.746(18)	W(24)-O(6)	1.710(18)

W(22)-O(77)	1.840(18)	W(23)-O(112)	1.828(16)	W(24)-O(54)	1.860(18)
W(22)-O(36)	1.866(18)	W(23)-O(64)	1.881(17)	W(24)-O(40)	1.896(18)
W(22)-O(58)	1.913(16)	W(23)-O(19)	1.915(17)	W(24)-O(113)	1.900(18)
W(22)-O(99)	1.939(18)	W(23)-O(13)	1.981(19)	W(24)-O(99)	1.918(17)
W(22)-O(35)	2.467(15)	W(23)-O(51)	2.402(16)	W(24)-O(35)	2.316(17)
W(25)-O(96)	1.739(19)	W(26)-O(48)	1.71(2)	W(27)-O(66)	1.72(2)
W(25)-O(109)	1.898(16)	W(26)-O(82)	1.847(16)	W(27)-O(3)	1.877(18)
W(25)-O(71)	1.909(18)	W(26)-O(41)	1.893(17)	W(27)-O(58)	1.920(16)
W(25)-O(68)	1.912(18)	W(26)-O(109)	1.926(16)	W(27)-O(79)	1.925(17)
W(25)-O(76)	1.930(18)	W(26)-O(83)	1.934(18)	W(27)-O(108)	1.943(18)
W(25)-O(43)	2.388(17)	W(26)-O(61)	2.438(17)	W(27)-O(4)	2.403(15)
W(28)-O(70)	1.741(18)	W(29)-O(92)	1.70(2)	W(30)-O(78)	1.73(2)
W(28)-O(111)	1.863(19)	W(29)-O(105)	1.842(17)	W(30)-O(103)	1.780(18)
W(28)-O(67)	1.880(16)	W(29)-O(100)	1.886(19)	W(30)-O(31)	1.892(15)
W(28)-O(98)	1.943(18)	W(29)-O(79)	1.947(16)	W(30)-O(44)	1.962(18)
W(28)-O(102)	1.949(19)	W(29)-O(40)	1.950(18)	W(30)-O(53)	2.041(17)
W(28)-O(22)	2.422(17)	W(29)-O(4)	2.397(15)	W(30)-O(45)	2.376(17)
As(1)-O(114)	1.638(18)	As(2)-O(45)	1.646(17)	As(3)-O(4)	1.655(15)
As(1)-O(101)	1.657(15)	As(2)-O(42)	1.680(17)	As(3)-O(59)	1.673(15)
As(1)-O(51)	1.661(16)	As(2)-O(61)	1.689(16)	As(3)-O(25)	1.680(17)
As(1)-O(22)	1.699(17)	As(2)-O(43)	1.705(16)	As(3)-O(35)	1.693(16)
Ce(1)-O(88)	2.372(17)	Ce(2)-O(21)	2.403(17)	Ce(3)-O(75)	2.382(17)
Ce(1)-O(103)	2.407(18)	Ce(2)-O(56)	2.415(17)	Ce(3)-O(110)	2.407(19)
Ce(1)-O(15)	2.457(18)	Ce(2)-O(80)	2.419(17)	Ce(3)-O(63)	2.448(17)
Ce(1)-O(27)	2.492(15)	Ce(2)-O(38)	2.488(16)	Ce(3)-O(73)	2.500(16)
Ce(1)-O(62)	2.536(17)	Ce(2)-O(94)	2.581(17)	Ce(3)-O(5)	2.558(17)
Ce(1)-OW2	2.583(17)	Ce(2)-OW3	2.586(19)	Ce(3)-O(47)	2.584(15)
Ce(1)-OW1	2.62(2)	Ce(2)-OW4	2.609(18)	Ce(3)-OW5	2.59(2)
Ce(1)-O(86)	2.66(2)	Ce(2)-O(2)	2.616(16)	Ce(3)-OW6	2.614(19)
Fe(1)-O(38)	1.917(17)	Fe(2)-O(1)	1.908(16)	Fe(3)-O(49)	1.905(17)
Fe(1)-O(32)	1.927(15)	Fe(2)-O(46)	1.931(17)	Fe(3)-O(27)	1.957(17)
Fe(1)-O(60)	1.959(18)	Fe(2)-O(73)	1.932(16)	Fe(3)-O(30)	1.978(16)
Fe(1)-O(2)	2.072(17)	Fe(2)-O(47)	2.083(16)	Fe(3)-O(86)	2.007(18)
Fe(1)-O(94)	2.103(16)	Fe(2)-O(5)	2.092(18)	Fe(3)-O(62)	2.118(17)
Fe(1)-O(101)	2.150(16)	Fe(2)-O(42)	2.108(17)	Fe(3)-O(25)	2.164(17)
K(2)-O(15)	3.167(18)	K(2)-O(30)	2.804(18)	K(2)-O(38)	3.339(18)
K(2)-O(46)	2.864(18)	K(2)-O(47)	2.809(17)	K(2)-O(60)	2.892(17)
K(2)-O(62)	2.803(17)	K(2)-O(80)	3.131(19)	K(2)-O(94)	2.819(18)
K(2)-O(110)	3.286(19)				
O(11)-W(1)-O(5)	102.6(8)	O(93)-W(2)-O(46)	104.6(8)	O(9)-W(3)-O(53)	104.1(8)
O(11)-W(1)-O(18)	100.9(8)	O(93)-W(2)-O(27)	101.3(7)	O(9)-W(3)-O(24)	100.3(8)
O(11)-W(1)-O(71)	104.9(8)	O(93)-W(2)-O(31)	102.3(7)	O(9)-W(3)-O(104)	103.2(8)
O(11)-W(1)-O(41)	100.1(8)	O(93)-W(2)-O(26)	96.5(7)	O(9)-W(3)-O(76)	100.4(9)
O(11)-W(1)-O(42)	172.2(8)	O(93)-W(2)-O(45)	173.5(7)	O(9)-W(3)-O(43)	170.0(7)
O(15)-W(4)-O(50)	103.8(8)	O(17)-W(5)-O(63)	103.4(9)	O(95)-W(6)-O(32)	104.8(8)

O(15)-W(4)-O(47)	96.1(7)	O(17)-W(5)-O(16)	101.6(8)	O(95)-W(6)-O(57)	103.7(8)
O(15)-W(4)-O(39)	89.5(8)	O(17)-W(5)-O(20)	102.7(9)	O(95)-W(6)-O(28)	100.6(8)
O(15)-W(4)-O(18)	158.9(8)	O(17)-W(5)-O(112)	93.9(8)	O(95)-W(6)-O(64)	97.8(7)
O(15)-W(4)-O(42)	87.9(7)	O(17)-W(5)-O(114)	172.2(8)	O(95)-W(6)-O(51)	167.8(7)
O(23)-W(7)-O(80)	103.1(8)	O(65)-W(8)-O(37)	102.3(7)	O(107)-W(9)-O(30)	104.1(8)
O(23)-W(7)-O(62)	103.7(8)	O(65)-W(8)-O(86)	104.1(8)	O(107)-W(9)-O(38)	100.2(8)
O(23)-W(7)-O(81)	100.2(8)	O(65)-W(8)-O(3)	101.8(8)	O(107)-W(9)-O(106)	96.9(8)
O(23)-W(7)-O(37)	97.8(7)	O(65)-W(8)-O(36)	98.9(7)	O(107)-W(9)-O(97)	101.1(8)
O(23)-W(7)-O(25)	168.9(7)	O(65)-W(8)-O(25)	174.7(7)	O(107)-W(9)-O(59)	170.5(7)
O(89)-W(10)-O(110)	104.7(8)	O(8)-W(11)-O(60)	104.7(8)	O(84)-W(12)-O(56)	102.2(8)
O(89)-W(10)-O(94)	102.1(8)	O(8)-W(11)-O(73)	100.1(8)	O(84)-W(12)-O(81)	104.7(8)
O(89)-W(10)-O(34)	102.1(7)	O(8)-W(11)-O(57)	96.2(8)	O(84)-W(12)-O(113)	102.8(8)
O(89)-W(10)-O(55)	97.6(7)	O(8)-W(11)-O(16)	103.0(8)	O(84)-W(12)-O(77)	96.6(8)
O(89)-W(10)-O(101)	167.0(7)	O(8)-W(11)-O(114)	173.1(8)	O(84)-W(12)-O(35)	165.1(7)
O(85)-W(13)-O(21)	102.7(9)	O(7)-W(14)-O(2)	101.3(8)	O(69)-W(15)-O(87)	98.7(8)
O(85)-W(13)-O(97)	100.4(8)	O(7)-W(14)-O(55)	102.1(8)	O(69)-W(15)-O(20)	101.8(8)
O(85)-W(13)-O(54)	103.2(8)	O(7)-W(14)-O(29)	102.4(8)	O(69)-W(15)-O(102)	100.8(8)
O(85)-W(13)-O(105)	94.8(8)	O(7)-W(14)-O(111)	101.9(8)	O(69)-W(15)-O(19)	103.1(7)
O(85)-W(13)-O(59)	173.0(7)	O(7)-W(14)-O(101)	172.5(7)	O(69)-W(15)-O(22)	169.8(7)
O(74)-W(16)-O(88)	104.1(8)	O(91)-W(17)-O(1)	103.7(8)	O(52)-W(18)-O(49)	103.4(8)
O(74)-W(16)-O(39)	102.4(8)	O(91)-W(17)-O(26)	105.2(8)	O(52)-W(18)-O(108)	99.8(8)
O(74)-W(16)-O(33)	102.9(7)	O(91)-W(17)-O(24)	99.1(8)	O(52)-W(18)-O(106)	105.3(8)
O(74)-W(16)-O(82)	94.6(8)	O(91)-W(17)-O(68)	100.0(8)	O(52)-W(18)-O(100)	99.5(8)
O(74)-W(16)-O(61)	164.0(7)	O(91)-W(17)-O(43)	167.6(8)	O(52)-W(18)-O(4)	168.2(8)
O(90)-W(19)-O(104)	101.1(8)	O(10)-W(20)-O(98)	102.6(9)	O(72)-W(21)-O(75)	103.1(8)
O(90)-W(19)-O(44)	102.8(9)	O(10)-W(20)-O(29)	101.7(8)	O(72)-W(21)-O(34)	104.4(7)
O(90)-W(19)-O(83)	100.6(9)	O(10)-W(20)-O(28)	102.2(8)	O(72)-W(21)-O(67)	95.5(8)
O(90)-W(19)-O(33)	101.0(8)	O(10)-W(20)-O(13)	101.0(9)	O(72)-W(21)-O(87)	102.1(8)
O(90)-W(19)-O(61)	170.2(8)	O(10)-W(20)-O(51)	171.8(8)	O(72)-W(21)-O(22)	163.9(7)
O(12)-W(22)-O(77)	102.1(9)	O(14)-W(23)-O(112)	103.8(8)	O(6)-W(24)-O(54)	102.9(8)
O(12)-W(22)-O(36)	103.4(8)	O(14)-W(23)-O(64)	100.9(8)	O(6)-W(24)-O(40)	101.1(8)
O(12)-W(22)-O(58)	102.5(8)	O(14)-W(23)-O(19)	101.5(8)	O(6)-W(24)-O(113)	100.1(8)
O(12)-W(22)-O(99)	102.1(9)	O(14)-W(23)-O(13)	98.9(8)	O(6)-W(24)-O(99)	100.6(8)
O(12)-W(22)-O(35)	169.8(8)	O(14)-W(23)-O(51)	170.9(8)	O(6)-W(24)-O(35)	169.9(7)
O(96)-W(25)-O(109)	101.3(8)	O(48)-W(26)-O(82)	100.6(8)	O(66)-W(27)-O(3)	103.0(9)
O(96)-W(25)-O(71)	103.2(8)	O(48)-W(26)-O(41)	103.6(8)	O(66)-W(27)-O(58)	103.7(8)
O(96)-W(25)-O(68)	100.3(8)	O(48)-W(26)-O(109)	101.0(8)	O(66)-W(27)-O(79)	101.5(9)
O(96)-W(25)-O(76)	101.6(8)	O(48)-W(26)-O(83)	101.3(8)	O(66)-W(27)-O(108)	101.6(9)
O(96)-W(25)-O(43)	170.9(7)	O(48)-W(26)-O(61)	169.8(7)	O(66)-W(27)-O(4)	170.6(7)
O(70)-W(28)-O(111)	102.8(9)	O(92)-W(29)-O(105)	104.9(8)	O(78)-W(30)-O(103)	103.5(9)
O(70)-W(28)-O(67)	102.1(8)	O(92)-W(29)-O(100)	101.9(9)	O(78)-W(30)-O(31)	100.2(8)
O(70)-W(28)-O(98)	102.3(8)	O(92)-W(29)-O(79)	101.4(8)	O(78)-W(30)-O(44)	103.1(8)
O(70)-W(28)-O(102)	100.7(8)	O(92)-W(29)-O(40)	100.7(9)	O(78)-W(30)-O(53)	95.7(8)
O(70)-W(28)-O(22)	169.9(8)	O(92)-W(29)-O(4)	172.3(8)	O(78)-W(30)-O(45)	173.1(7)
O(114)-As(1)-O(101)	111.5(8)	O(45)-As(2)-O(42)	109.7(9)	O(4)-As(3)-O(59)	111.8(7)

O(114)-As(1)-O(51)	111.6(8)	O(45)-As(2)-O(61)	111.5(8)	O(4)-As(3)-O(25)	108.0(8)
O(114)-As(1)-O(22)	111.9(9)	O(45)-As(2)-O(43)	111.8(8)	O(4)-As(3)-O(35)	107.8(8)
O(88)-Ce(1)-O(103)	80.5(6)	O(21)-Ce(2)-O(56)	83.0(6)	O(75)-Ce(3)-O(110)	71.9(6)
O(88)-Ce(1)-O(15)	73.5(6)	O(21)-Ce(2)-O(80)	127.3(6)	O(75)-Ce(3)-O(63)	81.7(6)
O(88)-Ce(1)-O(27)	128.6(5)	O(21)-Ce(2)-O(38)	75.3(6)	O(75)-Ce(3)-O(73)	128.8(5)
O(88)-Ce(1)-O(62)	141.3(6)	O(21)-Ce(2)-O(94)	132.1(5)	O(75)-Ce(3)-O(5)	152.9(6)
O(88)-Ce(1)-OW2	78.4(6)	O(21)-Ce(2)-OW3	139.1(6)	O(75)-Ce(3)-O(47)	141.4(5)
O(88)-Ce(1)-OW1	78.1(6)	O(21)-Ce(2)-OW4	71.8(6)	O(75)-Ce(3)-OW5	77.9(6)
O(88)-Ce(1)-O(86)	153.8(6)	O(21)-Ce(2)-O(2)	79.4(5)	O(75)-Ce(3)-OW6	80.0(6)
O(38)-Fe(1)-O(32)	104.1(7)	O(1)-Fe(2)-O(46)	91.3(7)	O(49)-Fe(3)-O(27)	106.1(7)
O(38)-Fe(1)-O(60)	99.4(7)	O(1)-Fe(2)-O(73)	102.2(7)	O(49)-Fe(3)-O(30)	90.9(7)
O(38)-Fe(1)-O(2)	91.7(7)	O(1)-Fe(2)-O(47)	167.4(7)	O(49)-Fe(3)-O(86)	93.2(7)
O(38)-Fe(1)-O(94)	85.1(7)	O(1)-Fe(2)-O(5)	91.7(7)	O(49)-Fe(3)-O(62)	167.6(7)
O(38)-Fe(1)-O(101)	158.3(7)	O(1)-Fe(2)-O(42)	95.0(7)	O(49)-Fe(3)-O(25)	94.1(7)

Table S3 Bond valence sum calculations of Ce, As and Fe for **1.**

Bonds	**Bond length (Å)**	**BVS***	**Bonds**	**Bond length (Å)**	**BVS***
Ce(1)-O(88)	2.372(17)	0.50	Ce(1)-O(62)	2.536(17)	0.32
Ce(1)-O(103)	2.407(18)	0.46	Ce(1)-OW2	2.583(17)	0.28
Ce(1)-O(15)	2.457(18)	0.40	Ce(1)-OW1	2.62(2)	0.26
Ce(1)-O(27)	2.492(15)	0.36	Ce(1)-O(86)	2.66(2)	0.23
$V_{Ce(1)}$ = **2.81**					
Ce(2)-O(21)	2.403(17)	0.46	Ce(2)-O(94)	2.581(17)	0.28
Ce(2)-O(56)	2.415(17)	0.45	Ce(2)-OW3	2.586(19)	0.28
Ce(2)-O(80)	2.419(17)	0.44	Ce(2)-OW4	2.609(18)	0.26
Ce(2)-O(38)	2.488(16)	0.37	Ce(2)-O(2)	2.616(16)	0.26
$V_{Ce(2)}$ = **2.80**					
Ce(3)-O(75)	2.382(17)	0.49	Ce(3)-O(5)	2.558(17)	0.30
Ce(3)-O(110)	2.407(19)	0.46	Ce(3)-O(47)	2.584(15)	0.28
Ce(3)-O(63)	2.448(17)	0.41	Ce(3)-OW5	2.59(2)	0.28
Ce(3)-O(73)	2.500(16)	0.35	Ce(3)-OW6	2.614(19)	0.26
$V_{Ce(3)}$ = **2.83**					
As(1)-O(114)	1.638(18)	1.42	As(2)-O(45)	1.646(17)	1.39
As(1)-O(101)	1.657(15)	1.35	As(2)-O(42)	1.680(17)	1.27
As(1)-O(51)	1.661(16)	1.33	As(2)-O(61)	1.689(16)	1.23
As(1)-O(22)	1.699(17)	1.20	As(2)-O(43)	1.705(16)	1.18
$V_{As(1)}$ = **5.30**			$V_{As(2)}$ = **5.07**		
As(3)-O(4)	1.655(15)	1.35			
As(3)-O(59)	1.673(15)	1.29			
As(3)-O(25)	1.680(17)	1.27			
As(3)-O(35)	1.693(16)	1.22			
$V_{As(3)}$ = **5.13**					
Fe(1)-O(38)	1.917(17)	0.65	Fe(1)-O(2)	2.072(17)	0.43
Fe(1)-O(32)	1.927(15)	0.64	Fe(1)-O(94)	2.103(16)	0.39
Fe(1)-O(60)	1.959(18)	0.58	Fe(1)-O(101)	2.150(16)	0.35
$V_{Fe(3)}$ = **3.04**					
Fe(2)-O(1)	1.908(16)	0.67	Fe(2)-O(47)	2.083(16)	0.42
Fe(2)-O(46)	1.931(17)	0.63	Fe(2)-O(5)	2.092(18)	0.41
Fe(2)-O(73)	1.932(16)	0.63	Fe(2)-O(42)	2.108(17)	0.39
$V_{Fe(3)}$ = **3.15**					
Fe(3)-O(49)	1.905(17)	0.67	Fe(3)-O(86)	2.007(18)	0.51
Fe(3)-O(27)	1.957(17)	0.59	Fe(3)-O(62)	2.118(17)	0.38
Fe(3)-O(30)	1.978(16)	0.55	Fe(3)-O(25)	2.164(17)	0.33
$V_{Fe(3)}$ = **3.03**					

* $V_M = \sum_j S_{M-O_j} = \sum_j \exp(\frac{r_0 - r_{M-O_j}}{0.37})$; $r_{CeIII\text{-}O}$ =2.116 Å; $r_{AsIII\text{-}O}$ = 1.767Å; $r_{FeIII\text{-}O}$ = 1.759Å. [ref 12].